 doi:10.20944/preprints201911.0243.v1

Article

Up-Down and Left-Right by the Heart Transcriptome

Sanda Iacobas [1], Bogdan Amuzescu [2] and Dumitru A Iacobas [3,4,*]

[1] Department of Pathology, New York Medical College, Valhalla, NY, U.S.A.; sandaiacobas@gmail.com
[2] Department Biophysics & Physiology, Faculty of Biology, University of Bucharest; bogdan@biologie.kappa.ro
[3] Personalized Genomics Laboratory, Center for Computational Systems Biology, Roy G. Perry College of Engineering, Prairie View A&M University, Prairie View, TX 77446, USA; daiacobas@pvamu.edu
[4] DP Purpura Department of Neuroscience, Albert Einstein College of Medicine, New York, NY, U.S.A.; dumitru.iacobas@einstein.yu.edu

* Correspondence: daiacobas@pvamu.edu; Tel.: +1(936) 261-9926

Abstract: Myocardium transcriptomes of mouse left and right atria and ventricles were profiled separately to identify the differences that might be responsible for the distinct functional roles of the four heart chambers. In total, 16,886 distinct unigenes have been quantified in all 16 samples collected from four adult male mice from the same litter. 15.76% of the quantified genes on the left and 16.5% on the right exhibited differential expression between the corresponding atrium and ventricle of the same side, while 5.8% in atria and 1.2% in ventricles were differently expressed between the left and the right. Beyond the differentially expressed genes, the study revealed distinct expression control and coordination of ion channels and genes within the cardiac muscle contraction, oxidative phosphorylation, glycolysis/glucogenesis, calcium and adrenergic signaling pathways. Interestingly, while expression of *Ank2* (encoding ankyrin-B) oscillates in phase with all its binding partners in the left ventricle, the percentage of synergistically expressed partners of *Ank2* is 15% and 37% in the left and right atria and 74% in the right ventricle. The analysis revealed also the high interventricular synchrony of the expression of ion channels.

Keywords: adrenergic signaling; ankyrin-B; calcium channel; calcium signaling; glycolysis; oxidative phosphorylation; potassium channel; sodium channel

1. Introduction

In all mammals and birds, the heart pumps the blood through the pulmonary circulation and the systemic circulation (that continue each-other) by the coordinated rhythmic contractions of its upper left and right atria (LA, RA) and lower left and right ventricles (LV, RV). Each of the four heart chambers has a well-defined role in circulation and the adequate morphology but how their distinct functions and buildups are determined by the transcriptomic profiles is still not completely understood.

In previous papers we have reported significant sex differences in the expression and networking of heart rhythm determinant genes (HRD) [1] and subcellular localization of HRD proteins [2]. We have also reported that mouse males have higher expression of HRD genes in atria than in ventricles, while mouse females have higher expression of HRD genes in ventricles than in atria [1].

There are important left-right differences in the mean arterial pressure between systemic and pulmonary circulation measured invasively in mice. The mean RV systolic pressure of 16.3 mm Hg [3] or 11.7 mm Hg [4] vs. mean LV systolic pressure of 96.2 mm Hg [3] or 107.7 mm Hg [4] lead to a five times greater LV workload compared to RV. There are also left-right differences in intraparietal tension, oxygen consumption and metabolic stress between the two ventricles, resulting in higher susceptibility to oxidative stress, reduced angiogenic response and higher likelihood of activation of cell death pathways with more rapid progression to failure of RV compared to LV [5].

A recent publication [6] compared the regulation of genes involved in atrial fibrillation (AF) from

 doi:10.20944/preprints201911.0243.v1

paired human left and right atrial appendages of healthy and AF patients, concluding that there are "different mechanisms for development, support and remodeling of AF within the left and right atria". Other authors compared the gene expressions from the left and right aortic arches of the chick embryo [7]. However, for technical reasons, none of these studies included a direct comparison of right/left expression levels in the same individual: [6] compared the regulations in AF patients with left or right appendages *vs*. healthy persons, while [7] performed comparisons of pooled samples from several embryos.

Differential gene expression studies based on both microarray and RNA sequencing methods have brought in recent years important contributions in understanding the complex landscape of heart embryogenesis [8], in defining signaling pathways involved in differentiation of heart regions [9], transcriptional enhancers and gene regulatory networks [10-12], involvement of miRNAs [13, 14], epigenetic reprogramming mechanisms [15] a.s.o.

A number of molecular mechanisms have been proposed in order to explain the left-right asymmetry at the level of the heart and generally in the internal organization of the amniote embryo. Starting from Kartagener's syndrome, a rare autosomal recessive disorder characterized by primary ciliary dyskinesia associated with *situs inversus* in about half of the human patients [16], researchers have proposed as primary left-right asymmetry determinant a mechanosensitive detection mechanism of unidirectional yolk sac fluid movement. The yolk sac fluid movement is generated by cilia rotation on the endoderm side of the primitive node, involving TRPP2 ion channels belonging to the polycystin subfamily of transient receptor potential (TRP), activation of non-canonical Hedgehog pathway and asymmetrical calcium signaling ([17], reviewed in [18-21]). Another rare clinical condition, the Holt-Oram syndrome, associated with congenital heart defects [22], has led to an elegant demonstration using differential gene expression methods of the rheostatic control exerted by the transcriptional activator Tbx5 in interventricular septum formation and ventricular patterning [23]. Other researchers have evidenced the role played by differential left-right expression of Nodal and bone morphogenetic (BMP) signaling pathways along the lateral plate mesoderm, leading to asymmetrical activation of transcription factors Pitx2 and Prrx1 and subsequent heart laterality in vertebrates by asymmetrical epithelial-to-mesenchymal transition [24]. Whole-cell patch-clamp studies on isolated cardiomyocytes have demonstrated the role of Notch1 signaling pathway in achievement of a mature shortened triangular ventricular action potential (AP) phenotype and the role played by various voltage-dependent K^+ channels (Kv) subunits and interacting proteins like KChIP2 [25].

The aim of our present study was to assess the differences of gene expression patterns in myocardium samples from the four heart chambers in adult male mice. We explored a number of functional pathways, addressing the differences in expression level, control and coordination between the two atria, the two ventricles, and atrium-ventricle on the same side and discuss why these differences are important for the heart function. A particular attention was given to the expression coordination of *Ank2* (encoding Ankyrin-B), a major player in cardiac physiology, with its potential binding partners [26] in each heart chamber. We studied also the expression coordination of the genes encoding ion channels and transporters (ICT) in each chamber as well as the synchronous expressions of the ICT genes between chambers.

2. Materials and Methods

2.1. Tissues

Four adult male C57Bl/6j mice, purchased from Charles River Laboratories International, Inc. (Wilmington, MA, USA) were used in this experiment to profile separately each heart atrium and ventricle from every mouse. The animals were housed in rooms with controlled temperature (22 ± 2°C) and humidity (55 ± 10%), continuous air flow and 12h light/12h dark cycle (6 am – 6 pm), were provided with normal rodent diet and water *ad libitum*, and monitored daily by trained veterinary personnel at Albert Einstein's Accredited Research Animal Care and Use Facility (https://www.einstein.yu.edu/research/shared-facilities/cores/52/animal-housing-and-studies). The

Preprints (www.preprints.org) | NOT PEER-REVIEWED | Posted: 20 November 2019 doi:10.20944/preprints201911.0243.v1

experiments were carried out according to the approved (#20100205) protocol (PI DA Iacobas) by the (Einstein) Institutional Animal Care & Use Committee (IACUC) for prevention of disease, daily observation and surveillance for assessment of animal health, and the methods of animal handling, restraint, anesthesia, and analgesia.

2.2. Microarray

The mice were decapitated under light isoflurane anesthesia and the hearts were isolated and perfused with saline to wash out all remaining blood. Total RNA was immediately extracted from as homogeneous as possible 1 – 2 mm pieces from each atrium and ventricle walls in separate vials with RNAEasy Minikit (Qiagen, Germantown, MD, USA), following manufacturer's instructions. RNA concentration was determined before and after reverse transcription in the presence of Cy3/Cy5 dUTP with a WU-83060-00 Thermo Scientific NanoDrop ND-1000 and its quality with a 2100 Bioanalyzer (Agilent, DE). The four groups of four samples each were marked as MAL (Male Atrium Left), MAR, MVL and MVR (Male Ventricle Right). 825 ng of differently (Cy3/Cy5) labeled biological replicas were hybridized 17h at 65°C with GPL10333 Agilent-026655 Whole Mouse Genome Microarray 4x44K v2. The chips were washed and scanned with an Agilent G2539A dual laser scanner at 5μm resolution in 20-bit scan mode and primary analysis performed with (Agilent) Feature Extraction 11.6 software.

2.3. Data analysis

We have used our standard protocol (e.g. [27]) for data filtration and normalization. Any spot with corrupted pixels or with foreground fluorescence less than twice the background in any of the 16 samples was removed from the analysis. As justified in a recent paper [28], profiling four biological replicas provides for each gene three independent measures: the average expression level, the expression variability and the expression coordination. The three features are as independent and complementary as are the impressions of a blind person and of a deaf one on the same movie.

2.3.1. Expression variability and control

Agilent gene expression microarrays probe redundantly the transcript abundances by not uniform (up to 28) numbers of spots. Therefore, we used the mid-interval chi-square estimate of the coefficient of variation (CV) of the normalized expression of each gene in the profiled tissue, adjusted for multiple spots, termed the Relative Expression Variability (REV):

$$REV_i^{(tissue)} = \underbrace{\frac{1}{2}\left(\sqrt{\frac{r_i}{\chi^2(r_i;0.975)}}+\sqrt{\frac{r_i}{\chi^2(r_i;0.025)}}\right)}_{\text{redundancy correction coefficient}}\sqrt{\sum_{k=1}^{R_i}\left(\frac{s_{ik}^{(tissue)}}{\mu_{ik}^{(tissue)}}\right)^2}_{CV_{ik}^{(tissue)}}\times 100\% \quad (1)$$

μ_{ik} = average expression level of gene i probed by spot k in the 4 biological replicas

s_{ki} = standard deviation of the expression level of gene i probed by spot k

$r_i = 4R_i - 1 =$ number of degrees of freedom

R_i = number of microarray spots probing redundantly transcript i, R_i = 1, 2, ..., 28

REV corrects the CV by a factor ranging from 1.566 (for R = 1) to 0.960 (R = 28).

REV was further used to compute the Relative Expression Control (REC) and the Pathway Relative Expression Control (PREC):

$$REC_i^{(tissue)} = \frac{\left\langle REV^{(tissue)}\right\rangle\Big|_{ALL}}{REV_i^{(tissue)}} - 1 \quad , \quad PREC_{\Gamma}^{(tissue)} = \frac{\left\langle REV^{(tissue)}\right\rangle\Big|_{ALL}}{\left\langle REV^{(tissue)}\right\rangle\Big|_{\Gamma}} - 1 \quad (2)$$

where higher positive *REC* values indicate genes whose expression level is strongly controlled by the cellular homeostatic mechanisms, presumably because their adequate expression level is critical for the cell survival, phenotypic expression or/and integration in the multicellular structure of the myocardium. By contrast, lower negative *REC*s are associated with less controlled genes that can easily

Preprints (www.preprints.org) | NOT PEER-REVIEWED | Posted: 20 November 2019 doi:10.20944/preprints201911.0243.v1

adapt to the slight fluctuations of the environmental conditions, as seen in the biological replicas. Similarly, high *PREC*s are associated with critically important pathways to preserve the phenotype against slight fluctuations of the environment and low *PREC*s with adapting pathways. One may observe that $PREC_{ALL}^{(tissue)} = \frac{\left\langle REV^{(tissue)} \right\rangle\Big|_{ALL}}{\left\langle REV^{(tissue)} \right\rangle\Big|_{ALL}} - 1 = 0$ sets the baseline for pathways comparison according to their *PREC* score.

2.3.2. Differential expression

A gene is considered as significantly differentially expressed between the compared tissues if the absolute expression ratio $|x|$ (x negative for down-regulation) exceeded the cut-off computed for that gene from its Relative Expression Variabilities (REV) in the two tissues:

$$\forall A, B, tissue = MAR, MAL, MVR, MVL$$

$$\left|x_i^{(A\to B)}\right| > CUT_i^{(A\to B)} = 1 + \sqrt{2\left(\left(REV_i^{(A)}\right)^2 + \left(REV_i^{(B)}\right)^2\right)} \quad , \quad where: \tag{3}$$

$$x_i^{(A\to B)} = \begin{cases} \sum_{k=1}^{R_i} \mu_{ik}^{(B)} \Big/ \sum_{k=1}^{R_i} \mu_{ik}^{(A)} & if \quad \sum_{k=1}^{R_i} \mu_{ik}^{(B)} \geq \sum_{k=1}^{R_i} \mu_{ik}^{(A)} \\ -\sum_{k=1}^{R_i} \mu_{ik}^{(A)} \Big/ \sum_{k=1}^{R_i} \mu_{ik}^{(B)} & if \quad \sum_{k=1}^{R_i} \mu_{ik}^{(B)} < \sum_{k=1}^{R_i} \mu_{ik}^{(A)} \end{cases}$$

In addition to the popular percentage of significantly regulated genes according to the above criterion (that replace the traditional uniform absolute fold-change cut-off of 1.5x or 2.0x), we quantify the alteration of the functional pathways by the Weighted Pathway Regulation (WPR), redefined from [30]:

$$WPR_{\Gamma}^{(A\to B)} = \overline{\left(wpr_i^{(A\to B)}\right)_{i\in\Gamma}} \quad , \quad where:$$

$$wpr_i^{(A\to B)} = \begin{cases} \mu_i^{(A)} \left(\left|x_i^{(A\to B)}\right| - CUT_i^{(A\to B)}\right)\left(1 - p_i^{(A\to B)}\right) & if \quad \left|x_i^{(A\to B)}\right| > CUT_i^{(A\to B)} \\ 0 & if \quad \left|x_i^{(A\to B)}\right| \leq CUT_i^{(A\to B)} \end{cases} \tag{4}$$

$p_i^{(A\to B)}$ = p-val of the heteroscedastic t-test of $\mu_i^{(B)} = \mu_i^{(A)}$

2.3.3. Expression coordination

Expression variability within biological replicas is used to compute the Pearson product-moment correlation coefficient between the ($\log_2$) expression of each gene with each other gene and identify ($p < 0.05$) significantly synergistically, antagonistically and independently expressed genes. The statistical significance of the correlation coefficient was determined with the publically available software https://www.youtube.com/watch?v=Kc3M5x7125A (two-tail *t*-test) for the degrees of freedom df = 4 (biological replicas)*R (number of spots probing redundantly each of the correlated transcripts) – 2. If each gene was probed by one spot, then df = 4 – 2 = 2, for two spots df = 8 - 2 = 6, for 3 spots df = 12 – 2 = 10. For unequal number of spots, we used for each biological replica the average expression level of all spots probing that gene.

Correlation results were further used to determine the differences of the gene networks among the four heart chambers. We used such analysis previously to determine the remodeling of gene networks in hearts of mice subjected to chronic constant or intermittent hypoxia [31, 32], with Chagas cardiomyopathy [30, 33], or with knocked-out expression of Cx43, the main gap junction protein in cardiomyocytes [34].

Profiling the transcriptomes of all heart chambers from the same animal gives the possibility to test whether the genes encoding interesting proteins (like ion channels and transporters) are expressed in synchrony. We consider a gene as synchronously expressed in two heart chambers if its expression

Preprints (www.preprints.org) | NOT PEER-REVIEWED | Posted: 20 November 2019 doi:10.20944/preprints201911.0243.v1

levels in these two chambers fluctuates in phase (positive Pearson correlation coefficient) among the biological replicas collected from the same animals.

2.4. Pathway analysis

Gene Ontology Consortium (www.geneontology.org) and/or Kyoto Encyclopedia for Genes and Genomes (https://www.kegg.jp) were used to select the genes encoding ion channels and transporters (ICT, 185 genes) and genes involved in the following pathways: adrenergic signaling in cardiomyocytes (ASC, mmu04261, 104 genes), calcium signaling (CAS, mmu04020, 121 genes), cardiac muscle contraction (CMC, mmu04260, 65 genes), glycolysis/gluconeogenesis (GLY, mmu00010, 50 genes) and oxidative phosphorylation (OP, mmu00190, 111 genes).

3. Results

Raw and processed microarray data have been deposited and are publically available at https://www.ncbi.nlm.nih.gov/geo/ as GSE45339 and GSE45348. After replacing the results from each group of spots probing redundantly the same transcript with the average expression level in the group, we arrived with a total of 16,886 unigenes adequately quantified in each of the four chambers from all mice.

3.1. Differential expression and control of selected pathways and groups of genes among heart chambers

Figure 1 presents the percentages of the differentially expressed genes, the Weighted Pathway Regulations (WPR) and Pathway Relative Expression Control (PREC) of the selected pathways. The scores of all quantified genes (ALL) were included for comparison. While significant differences between the atrium and the ventricle from the same side of the heart were expected, of note are the large differences between the two atria and the very small differences between the two ventricles.

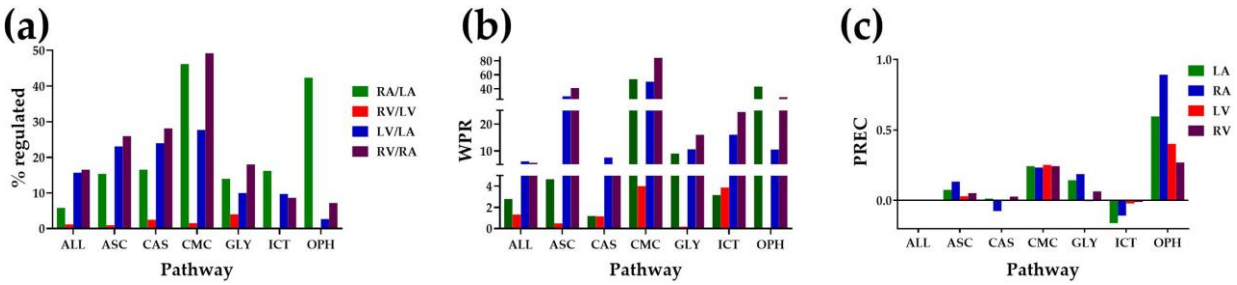

Figure 1: Differential expression, control and coordination of selected functional pathways and groups of genes. **(a)** Percentages of regulated genes. **(b)** Weighted Pathway Regulation (WPR). **(c)** Pathway Relative Expression Control. **ALL** = all genes, **ASC** = adrenergic signaling in cardiomyocytes, **CAS** = calcium signaling, **CMC** = cardiac muscle contraction, **GLY** = glycolysis/gluconeogenesis, **ICT** = ion channels and transporters, **OPH** = oxidative phosphorylation. Note that CMC is the most altered, OPH the most controlled and ICT the least controlled pathway.

3.2. Chamber specificity of gene expression within functional pathways

Figures 2-5 present the differentially expressed genes within the adrenergic signaling, calcium signaling, glycolysis/gluconeogenesis and oxidative phosphorylation pathways between the two atria, between the two ventricles (when relevant) and between the ventricles and atria of the same side. Appendix Figure A1 presents the differentially expressed genes within the cardiac muscle contraction and Figure A2 those within the adrenergic signaling pathway between the two atria and between the atrium and the ventricle of each side of the heart.

Preprints (www.preprints.org) | NOT PEER-REVIEWED | Posted: 20 November 2019 doi:10.20944/preprints201911.0243.v1

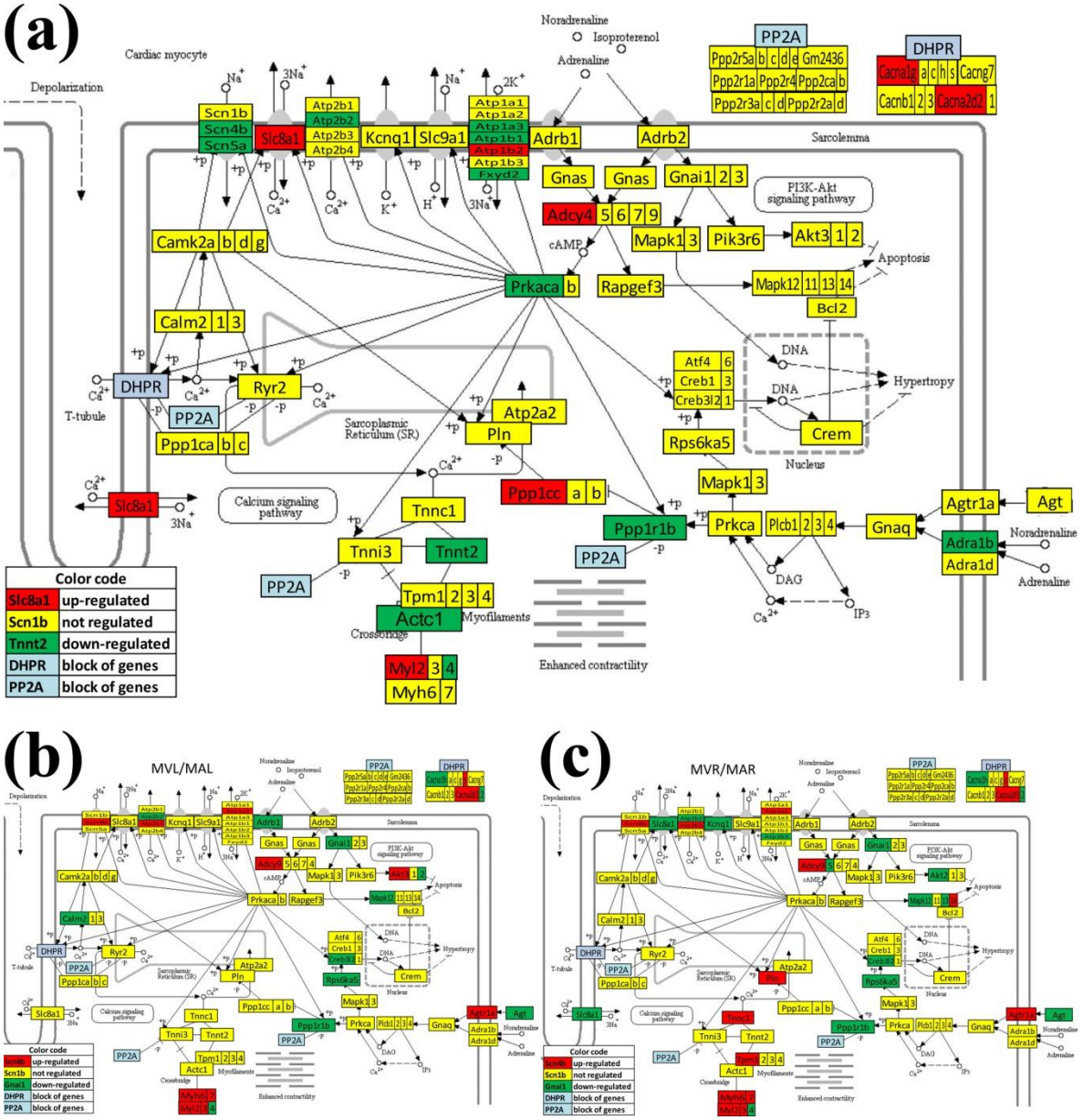

Figure 2: KEGG map (mmu04261) of the differential expression of adrenergic signaling in cardiomyocytes (ASC) genes in: **(a)** the right atrium with respect to the left atrium, **(b)** the left ventricle vs left atrium and (c) right ventricle vs right atrium. Only *Akt3* was found with significant lower expression in the right ventricle with respect the left one. Red/green/yellow background of gene symbol indicates up-/down-/not regulated. **Genes with significant differences:** actin alpha cardiac muscle 1 (*Actc1*), adenylate cyclases (*Adcy4*, *Adcy5*, *Adcy9*), adrenergic receptor alpha 1b (*Adra1b*), adrenergic receptor beta 1 (*Adrb1*), angiotensin II receptor type 1a (*Agtr1a*), angiotensinogen (*Agt*), thymoma viral proto-oncogenes (*Akt2*, *Akt3*), Ca^{++} transporting ATPases (*Atp2b2*, *Atp2b3*), Na^{+}/K^{+} transporting ATPases (*Atp1a2*, *Atp1a3*, *Atp1b1*, *Atp1b2*), calcium channels (*Cacna1g*, *Cacna1h*, *Cacna1s*, *Cacna2d1*, *Cacna2d2*), calmodulin 2 (*Calm2*), cAMP responsive element binding protein 3-like 2 (*Creb3l2*), FXYD domain-containing ion transport regulator 2 (*Fxyd2*), potassium voltage-gated channel subfamily Q member 1 (*Kcnq1*), mitogen-activated protein kinases (*Mapk12*, *Mapk13*, *Mapk14*), myosins (*Myh6*, *Myh7*, *Myl2*, *Myl3*, *Myl4*), phospholamban (*Pln*), protein phosphatase 1 regulatory (inhibitor) subunit 1B (*Ppp1r1b*), protein kinase C, alpha (*Prkca*), ribosomal protein S6 kinase polypeptide 5 (*Rps6ka5*), sodium channel type IV beta (*Scn4b*), sodium channel voltage-gated type V alpha (*Scn5a*), solute carrier family 8 (sodium/calcium exchanger) member 1 (*Slc8a1*), troponins (*Tnnc1*, *Tnnt1*) and tropomyosin 1 alpha (*Tpm1*).

Preprints (www.preprints.org) | NOT PEER-REVIEWED | Posted: 20 November 2019 doi:10.20944/preprints201911.0243.v1

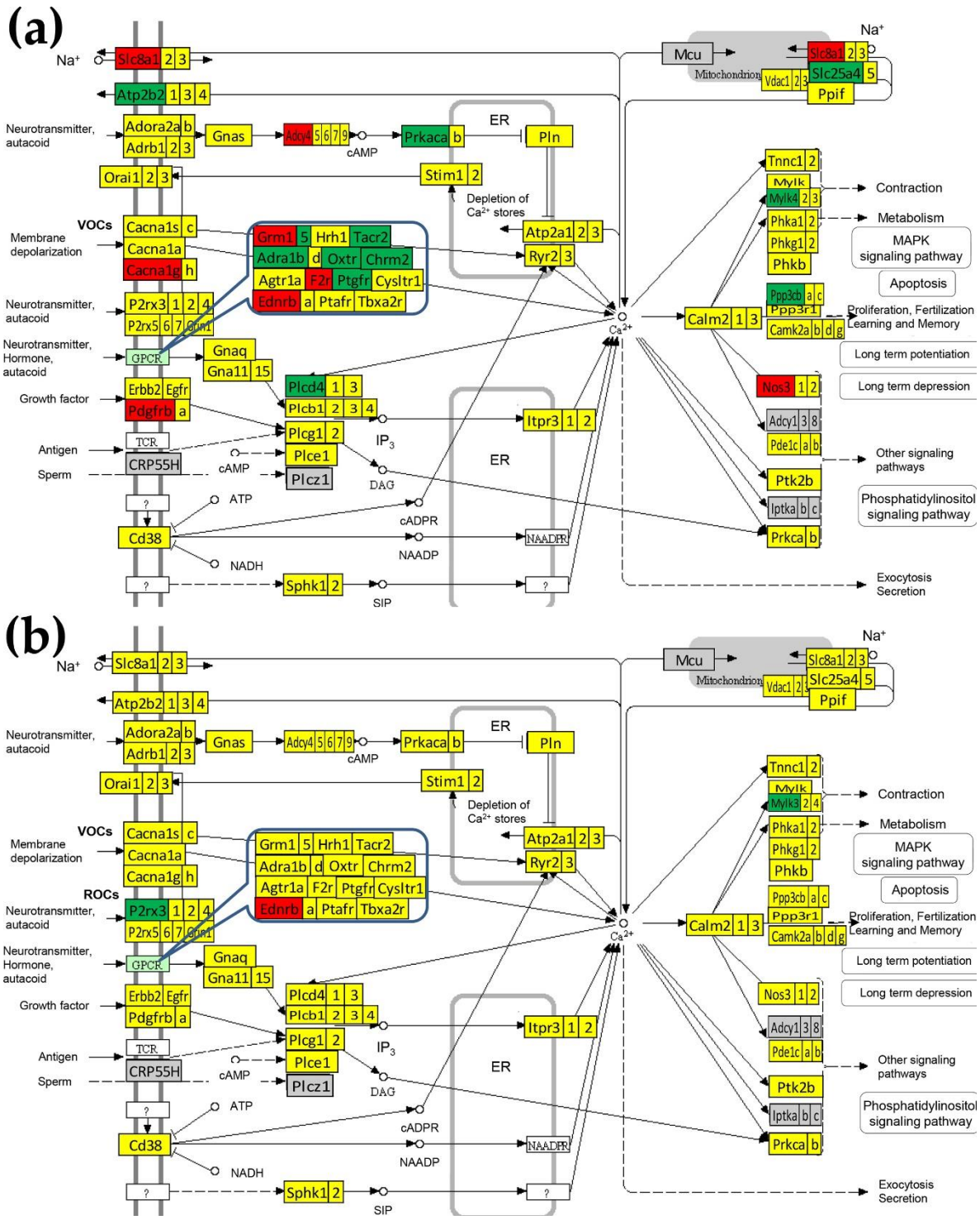

Preprints (www.preprints.org) | NOT PEER-REVIEWED | Posted: 20 November 2019 doi:10.20944/preprints201911.0243.v1

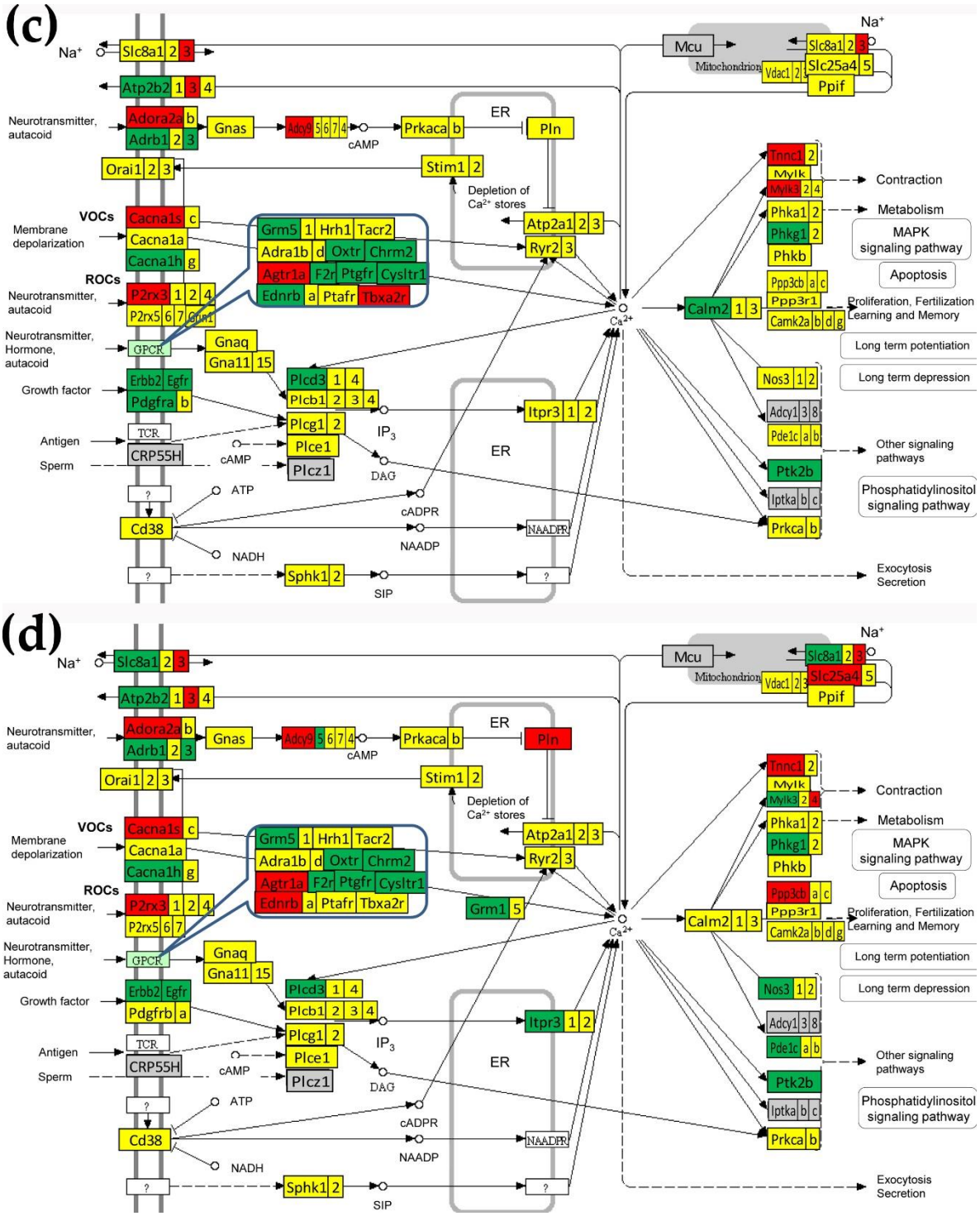

Figure 3: KEGG map (mmu04020) of the differential expression of calcium signaling (CAS) genes in: **(a)** the right atrium with respect to the left atrium, **(b)** right ventricle vs left ventricle, **(c)** left ventricle vs left atrium, **(d)** right ventricle vs right atrium. Red/green/yellow background of gene symbol indicates up-/down-/not regulated. **Genes with significant differences:** *Adcy4*, *Adcy5*, *Adcy9*, adenosine A2a receptor (*Adora2a*), adrenergic receptors (*Adra1b*, *Adrb1*, *Adrb3*), *Agtr1a*, *Atp2b2*, *Atp2b3*, *Cacna1g*, *Cacna1h*, *Cacna1s*, *Calm2*, cholinergic receptor muscarinic 2 cardiac (*Chrm2*), cysteinyl leukotriene receptor 1 (*Cysltr1*), endothelin receptor type B (*Ednrb*), epidermal growth factor receptor (*Egfr*), v-erb-b2 erythroblastic leukemia viral oncogene homolog 2 (*Erbb2*), coagulation factor II (thrombin) receptor (*F2r*), metabotropic glutamate receptors (*Grm1*, *Grm5*), inositol 1,4,5-triphosphate receptor 3 (*Itpr3*), myosin light chain kinases (*Mylk3*, *Mylk4*), nitric oxide synthase (*Nos2*, *Nos3*), oxytocin receptor (*Oxtr*), purinergic receptor P2X ligand-gated ion channel 3 (*P2rx3*), phosphodiesterase 1C (*Pde1c*), platelet

 doi:10.20944/preprints201911.0243.v1

derived growth factor receptors (*Pdgfra, Pdgfrb*), phosphorylase kinase gamma 1 (*Phkg1*), phospholipases (*Plbd1, Plcd3, Plcd4*), phospholamban (*Pln*), protein phosphatase 3, catalytic subunit, beta isoform (*Ppp3cb*), protein kinase cAMP dependent catalytic alpha (*Prkaca*), prostaglandin F receptor (*Ptgfr*), PTK2 protein tyrosine kinase 2 beta (*Ptk2b*), solute carriers (*Slc25a4*, *Slc8a1, Slc8a3*), tachykinin receptor 2 (*Tacr2*), thromboxane A2 receptor (*Tbxa2r*) and troponin C cardiac/slow skeletal (*Tnnc1*).

Preprints (www.preprints.org) | NOT PEER-REVIEWED | Posted: 20 November 2019 doi:10.20944/preprints201911.0243.v1

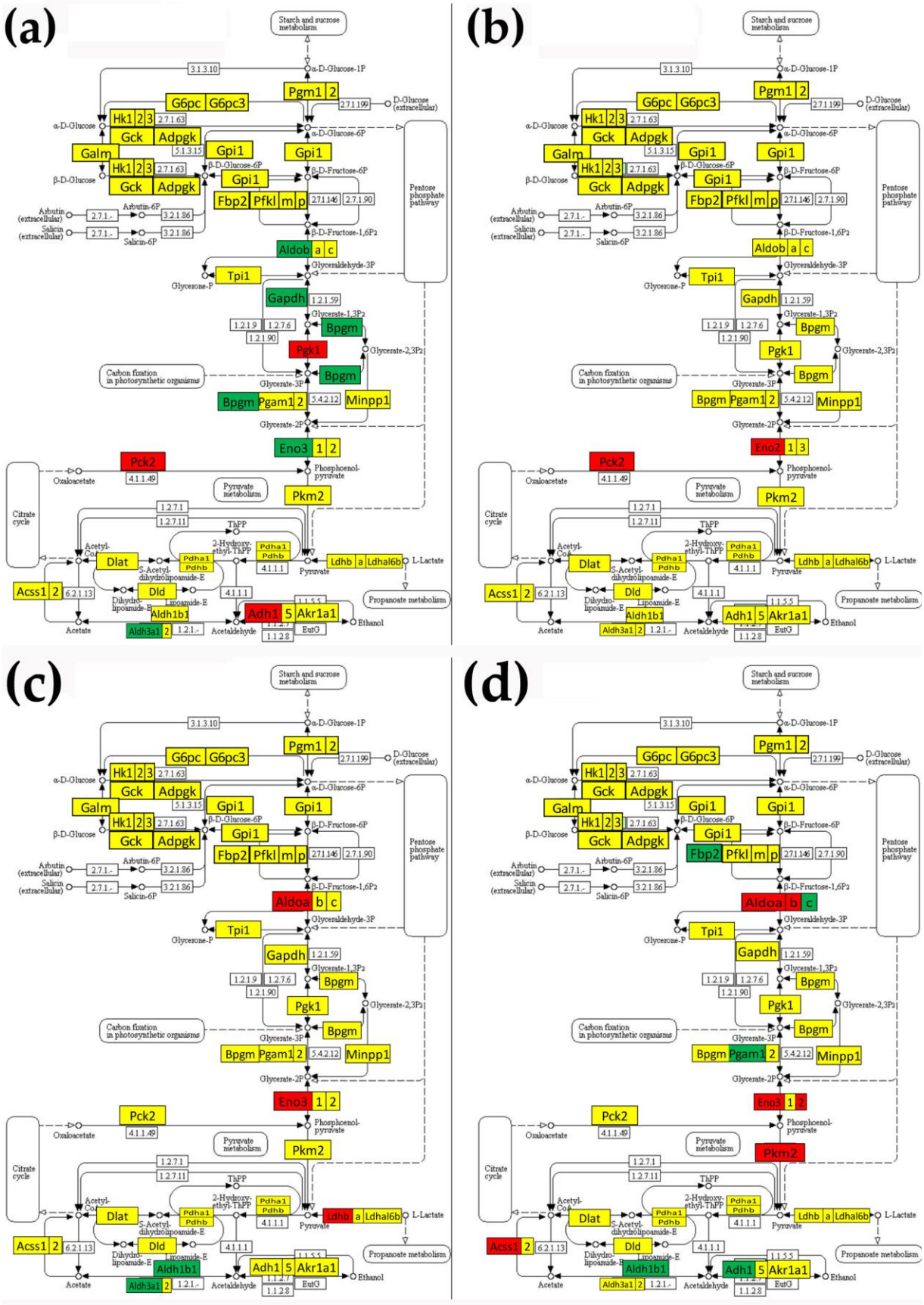

Figure 4: KEGG map (mmu00010) of the differential expression of glycolysis/gluconeogenesis (GLY) genes in: **(a)** the right atrium with respect to the left atrium, **(b)** right ventricle vs left ventricle, **(c)** left ventricle vs left atrium, **(d)** right ventricle vs right atrium. Red/green/yellow background of gene symbol indicates up-/down-/not regulated. **Genes with significant differences:** acyl-CoA synthetase

Preprints (www.preprints.org) | NOT PEER-REVIEWED | Posted: 20 November 2019 doi:10.20944/preprints201911.0243.v1

short-chain family member 1 (*Acss1*), alcohol dehydrogenase 1 (*Adh1*), aldehyde dehydrogenases (*Aldh1b1, Aldh3a1*), aldolases (*Aldoa, Aldob, Aldoc*), 2,3-bisphosphoglycerate mutase (*Bpgm*), enolase 3 beta muscle (*Eno3*), fructose bisphosphatase 2 (*Fbp2*), glyceraldehyde-3-phosphate dehydrogenase (*Gapdh*), phosphoenolpyruvate carboxykinase 2 (*Pck2*), phosphoglycerate mutase 1 (*Pgam1*) and pyruvate kinase muscle (*Pkm2*).

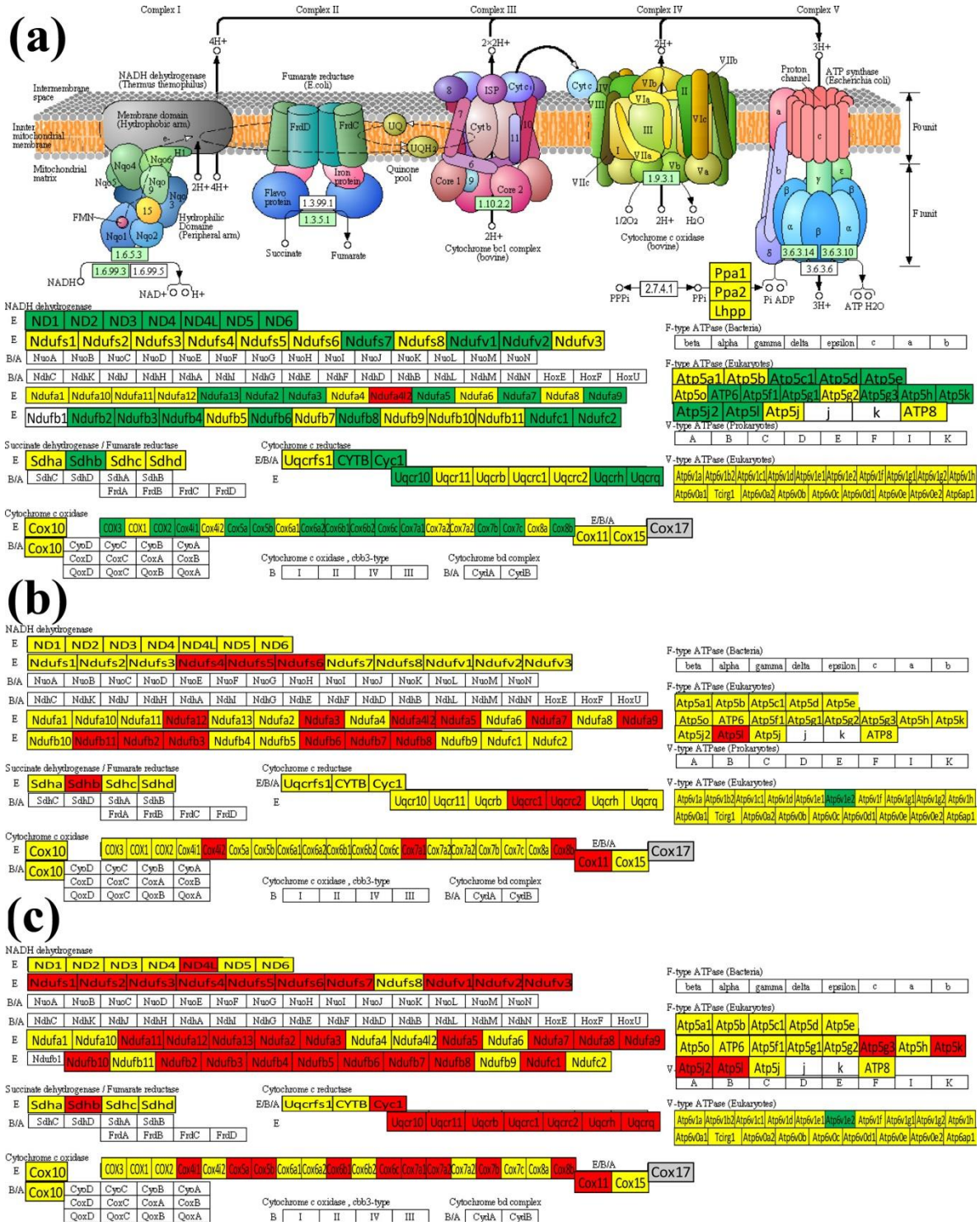

Figure 5: KEGG map (mmu00190) of the differential expression of oxidative phosphorylation (OPH) genes in: **(a)** the right atrium with respect to the left atrium, **(b)** left ventricle vs left atrium and **(c)** right ventricle vs right atrium. No significant difference was found between the expressions of OPH genes in the two ventricles.

Preprints (www.preprints.org) | NOT PEER-REVIEWED | Posted: 20 November 2019 doi:10.20944/preprints201911.0243.v1

3.3. Expression correlation and synchrony of ion channels and transporters

Figure 6 presents examples of significantly (p-val < 0.05) synergistically, antagonistically and independently expressed ICT genes, the percentages of the significant synergistic expressions of the ICT genes with each-other in each chamber and of the same ICT genes between two chambers.

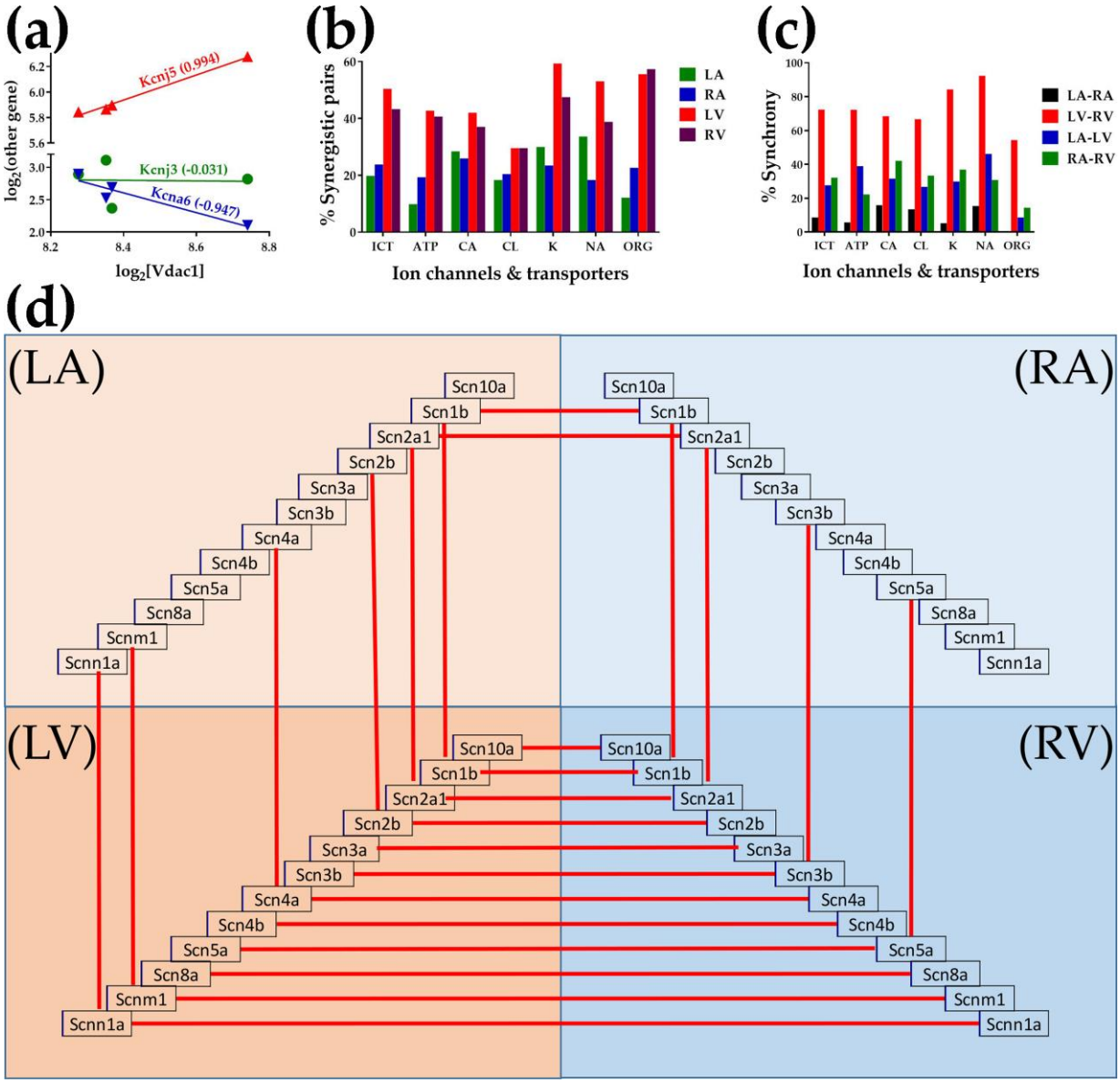

Figure 6: Correlation of the expressions of genes encoding ion channels and transporters (ICT). **(a)** Examples of synergistically (*Kcnj5* = potassium inwardly-rectifying channel, subfamily J, member 5), antagonistically (*Kcna6* = potassium voltage-gated channel, shaker-related, subfamily, member 6) and independently (*Kcnj3* = potassium inwardly-rectifying channel, subfamily J, member 3) expressed genes with *Vdac1* (voltage-dependent anion channel 1) in the left atrium. **(b)** Percentage of synergistically expressed ion channel and transporter gene pairs within each chamber. The correlation was computed for each ICT gene with each other ICT gene within the same chamber. **ICT** = percentage out of all 17,020 pairs that can be formed with the quantified ICT genes, **ATP** = transporting ATPases (1,378 pairs), **ORG** = transporters through organelle (mitochondria, lysosomes) membranes (903 pairs), **CA** = calcium channels (153 pairs), **CL** = chloride channels (91 pairs), **NA** = sodium channels (91 pairs), **K** = potassium channels (1,596 pairs)**.** Note the significantly larger percentages of synergistically expressed pairs of ion channels and transporters in the ventricles. **(c)** Synchronous expressions of ICT

Preprints (www.preprints.org) | NOT PEER-REVIEWED | Posted: 20 November 2019 doi:10.20944/preprints201911.0243.v1

genes between two chambers. **(d)** Synchronous expressions of sodium channels in paired heart chambers.

Figure 7 shows the significantly (p-val < 0.05) synergistically, antagonistically and independently expressed pairs out of the 2,793 pairs formed by the 57 potassium channel genes with the 49 sodium, calcium and chloride channel genes, in the four chambers of the male mouse heart. While there are less than 1% significant antagonistic and independent pairs, the percentages of the synergistically expressed pairs are very high in all chambers, although with remarkable differences among them: 28% in the LA, 22% in the RA, 53% in the LV and 43% in the RV.

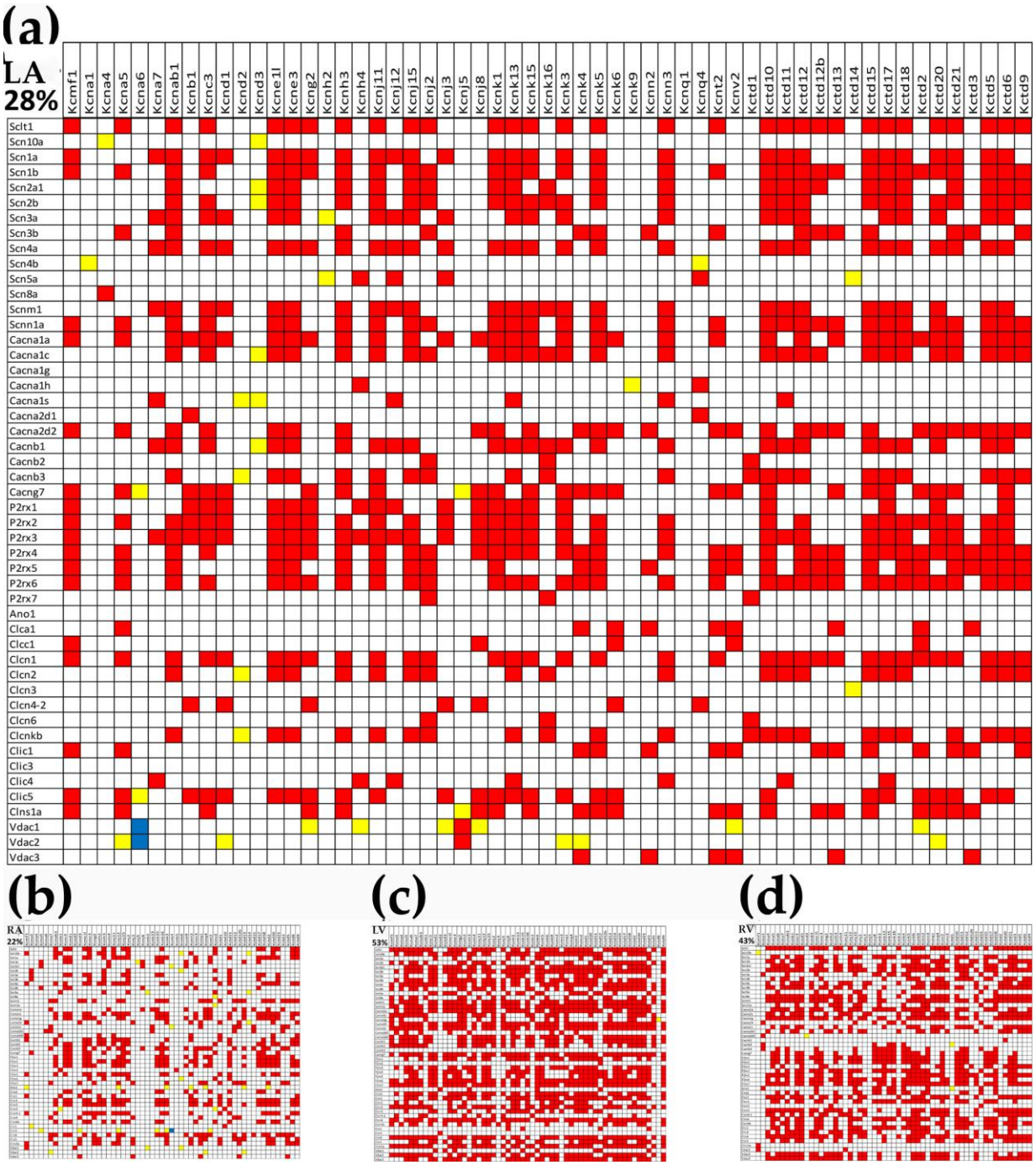

Figure 7: Significant (p < 0.05) expression correlation and independence of the 57 potassium channel genes with the 49 sodium, calcium and chloride channel genes in **(a)** left atrium, **(b)** right atrium, **(c)** left ventricle, **(d)** right ventricle. Red/blue/yellow square indicates that the potassium channel gene

Preprints (www.preprints.org) | NOT PEER-REVIEWED | Posted: 20 November 2019 doi:10.20944/preprints201911.0243.v1

labeling the column and the sodium/calcium/chloride channel labeling the intersected raw are significantly synergistically/antagonistically/ independently expressed.

3.4. Expression coordination of Ankyrin B with its potential binding partners

Ankyrin-B (encoded by *Ank2*) is an essential cytoskeletal component that performs integral transmembrane protein anchoring, containing four primary domains: a membrane-binding domain, a spectrin-binding domain, a death domain, and a C-terminal domain, each with binding partners discussed in a recent paper [34]. Pearson correlation coefficients between the expression levels of *Ank2* and those of its potential binding partners were computed for each chamber. The analysis aimed to validate the partners whose transcripts abundances oscillate in phase with that of *Ank2* among biological replicas to satisfy the "transcriptomic stoichiometry" [27].

Figure 8 presents the significant expression coordination between the expression levels of *Ank2*, a major player in the cardiac physiology, with its potential binding partners [26] in the four heart chambers. While no statistically significant antagonism or independence was found, the percentages of significant synergisms were very different: 12% in the left atrium, 40% in the right atrium, 100% in the left ventricle and 72% in the right ventricle.

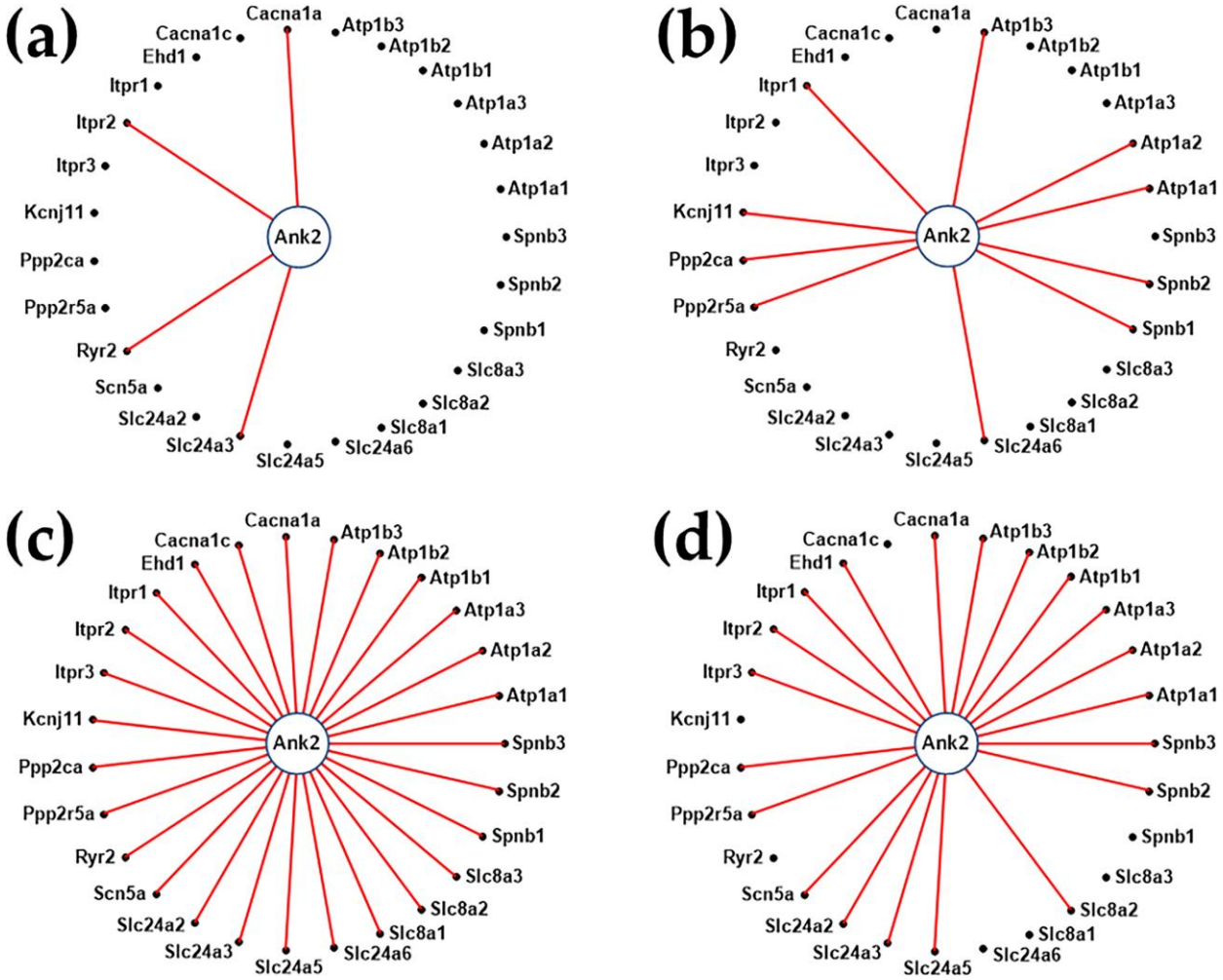

Figure 8: Expression coordination of *Ank2* with its known binding partners in **(a)** left atrium, **(b)** right atrium, **(c)** left ventricle, **(d)** right ventricle. **Genes:** *Atp1a1/2/3* (ATPase, Na+/K+ transporting, alpha 1/2/3 polypeptide), *Atp1b1/2/3* (ATPase, Na+/K+ transporting, beta 1/2/3 polypeptide), *Cacna1a* (calcium channel, voltage-dependent, P/Q type, alpha 1A subunit), *Cacna1c* (calcium channel, voltage-dependent, L type, alpha 1C subunit), *Ehd1* (EH-domain containing 1), *Itpr1/2/3* (inositol 1,4,5-trisphosphate receptor 1/2/3), *Kcnj11* (potassium inwardly rectifying channel, subfamily J, member 11), *Ppp2ca* (protein phosphatase 2 (formerly 2A), catalytic subunit, alpha isoform), (protein phosphatase 2,

 doi:10.20944/preprints201911.0243.v1

regulatory subunit B (B56), alpha isoform), *Ryr2* (ryanodine receptor 2, cardiac), *Scn5a* (sodium channel, voltage-gated, type V, alpha), *Slc24a2/3/5/6* (solute carrier family 24 (sodium/potassium/ calcium exchanger), member 2/3/5/6), *Slc8a1/2/3* (solute carrier family 8 (sodium/calcium exchanger), member 1/2/3), *Spnb1/2/3* (spectrin beta 1/2/3).

4. Discussion

The present study revealed a number of statistically significant differences in the transcriptomic profiles of the myocardial tissue from the four heart chambers of male adult C57Bl/6j mice in good health condition. The differences were larger between the atrium and ventricle of same side, as well as between the right and left atria, than between the right and left ventricles, both in terms of the overall expression levels and for the specific regulatory pathways selected for analysis. The differences between the right and the left atria (RA/LA) were more prominent for the cardiac muscle contraction (CMC) and oxidative phosphorylation (OPH) pathways, amounting to over 40% of differentially expressed genes.

The most logical explanation for these differences, and particularly for the surprisingly small differences between the right and the left ventricle (RV/LV), resides in the evolution of the cardiovascular system. Thus, the initial separation of the contracting vessel into one atrium and one ventricle, present since the beginning of the chordate phylum, was followed by the separation into right and left atria that started with amphibians, and right and left ventricle with the archosaurs (crocodilians and birds, including all extinct dinosaurs, crocodilian relatives and pterosaurs). It must be also understood that the right and left ventricle have different embryogenetic origins: LV and part of the atria arise from the early heart tube, in turn developed from the first heart field, an area of anterior splanchnic mesoderm formed early during gastrulation, while RV, the outflow tract and the main parts of atrial tissue arise from the second heart field that coalesces with the heart tube at its arterial and venous edges, being derived from the pharingeal mesoderm and dorsal mesocardium [35].

The major drivers during heart embryogenesis were determined by principal component analysis (PCA) of microarray data from samples taken at different developmental stages [8, 9]. Differential gene expression revealed by microarray data analysis was also used to prove that the anterior intestinal portal endoderm functions as a heart organizer, being capable to induce cardiac identity into non-cardiac mesoderm even if heterotopically transplanted, and patterning cardiac tissue to express ventricular and suppress atrial region identifiers [36]. Moreover, single-cell RNA-seq was used to understand the earliest steps of cardiovascular lineage differentiation, analyzing MesP1-positive cardiovascular progenitor cells and different cardiac progenitor populations corresponding to the first and second heart fields at embryonic day E6.5 and E7.25, respectively, in mice [37, 38].

The complex regulation of cardiomyocyte differentiation involves a complex interplay of signaling pathways and gene regulatory networks [9], families of activatory transcription factors [11], transcription enhancers [12, 39] and epigenetic mechanisms [10, 15]. The analysis of differential gene expression in our dataset for the adrenergic signaling in cardiomyocytes and calcium signaling pathways revealed important differences between the atrium and ventricle on the same side, as expected, given the important regulatory functions of these pathways within cardiac physiology. But the significant differences in expression between atria and ventricles were not found for the β-adrenergic receptor genes themselves; they were rather found for associated membrane proteins involved in ion transport as effectors, such as subunits of the Na^+/K^+ pumps, Na^+/Ca^{2+} exchangers (NCX), L-type Ca^{2+} channel and voltage-dependent Na^+ channel subunits, the angiotensin II receptor type Ia (*Agtr1a*), or regulatory protein kinases such as *Akt3*, involved in cell signaling in response to insulin and growth factors (Figure 2b,c). These results are relevant in the light shed recently by studies assessing the important roles of adrenergic signaling and internal calcium dynamics in the "fight-or-flight" response to sympathetic nerve stimulation, achieving via species-specific fine-tuning of these processes the required positive inotropic response to stress-generating situations [40].

Although the RNA was extracted from as homogeneous as possible tissue samples, the analysis provides the average expression levels for the variety of cells composing the myocardium: cardiomyocytes, fibroblasts, endothelial and smooth muscle cells, stem cell niches and supporting cells,

 doi:10.20944/preprints201911.0243.v1

nerve endings, immune system cells, etc. However, as we proved in previous publications [41, 42], the transcriptome of each cell type is strongly modeled by the heterogeneous cellular environment, so that profiling each cell phenotype separately will give also a false picture. Therefore, we were particularly interested in genes expressed exclusively at cardiomyocyte level, such as those encoding different subunits of certain cardiac-specific voltage-dependent ion channels and transporters. Table S1 of the Appendix lists the ratios of expression at mRNA level between right and left ventricle (RV/LV) and right and left atria (RA/LA) for 12 genes encoding subunits of cardiac-specific ion channels and transporters. A highly relevant finding revealed by our detailed analysis methods is represented by the negative Pathway Relative Expression Control (PREC) values for the ion channels and transporters (ICT) group of genes and calcium signaling pathway for right atrium compared to positive values for other functional pathways, as shown in Figure 1c, which signifies that ion channels and transporters genes' expression levels are very tightly controlled owing to their extremely important roles in shaping cardiomyocyte action potentials in different heart chambers. Similar findings strengthening this conclusion are the high percentages of synergistic pairs (particularly for the left ventricle) and gene expression synchrony (particularly for RV vs LV) for different families of ion channels and transporters, as well as the high percentages of correlated gene expression between *Ank2* and its interacting partners in the ICT group, amounting up to 100% for the left ventricle.

Several putative molecular mechanisms have been proposed and explored to explain the right/left asymmetry in heart formation and function. One interesting hypothesis emphasizes the role of *Pkd2* (polycystin 2, transient receptor potential cation channel), belonging to the polycystin subgroup of the transient receptor potential (TRP) family, in sensing the leftward flow of fluid in the yolk sack produced by unidirectional rotation of cilia on the endodermic surface of the Hensen node [17]. Another theory claims that differential ion channel activity in early embryo cells leads to unidirectional mRNA flow via gap junctions and subsequently to asymmetrical gene expression. An elegant proof-of-concept studies [22] proved that the T-box transcription factor *Tbx5* exerts a "rheostatic" control on expression levels of multiple genes including a network of cardiac transcription factors, cell signaling molecules involved in development, and ion channel proteins, all contributing to interventricular septum formation and right-left ventricle asymmetry [22, 23].

5. Conclusions

We can conclude that the up-down and left-right asymmetries in myocardial structure and function result from complex and strictly controlled gene-regulated processes that can be perturbed in pathological situations.

Supplementary Materials: The following are available online, Figure A1: KEGG map (mmu04260) of the differential expression of cardiac muscle contraction (CMC) genes in: (a) the right atrium with respect to the left atrium, (b) left ventricle vs left atrium and (c) right ventricle vs right atrium, Figure A2: KEGG map (mmu04261) of the differential expression of adrenergic signaling in cardiomyocytes (ASC) genes in the right ventricle with respect to the right atrium. Table S1: Ratios of RV/LV and RA/LA gene expression in our study for 12 genes encoding subunits of cardiac ion channels and transporters

Author Contributions: conceptualization, D.A.I. and B.A.; methodology, S.I. and D.A.I.; software, D.A.I.; validation, S.I., B.A. and D.A.I.; formal analysis, D.A.I.; investigation, S.I.; resources, D.A.I..; data curation, B.A. and D.A.I.; writing—original draft preparation, D.A.I. and B.A.; visualization, B.A. and D.A.I.; supervision, D.A.I.; project administration, D.A.I.; funding acquisition, D.A.I.

Funding: This research was funded in part by the Texas A&M University System Chancellor's Research Initiative (CRI) for the Center for Computational Systems Biology at Prairie View University (D.A.I.) and by the National Institutes of Health, grant number 5R01HL092001 (D.A.I.) B.A. acknowledges funding from Competitiveness Operational Programme 2014–2020 project P_37_675 (contract no. 146/2016), Priority Axis 1, Action 1.1.4, co-financed by the European Funds for Regional Development and Romanian Government funds.

Acknowledgments:

Conflicts of Interest: The authors declare no conflict of interest.

Preprints (www.preprints.org) | NOT PEER-REVIEWED | Posted: 20 November 2019 doi:10.20944/preprints201911.0243.v1

Appendix

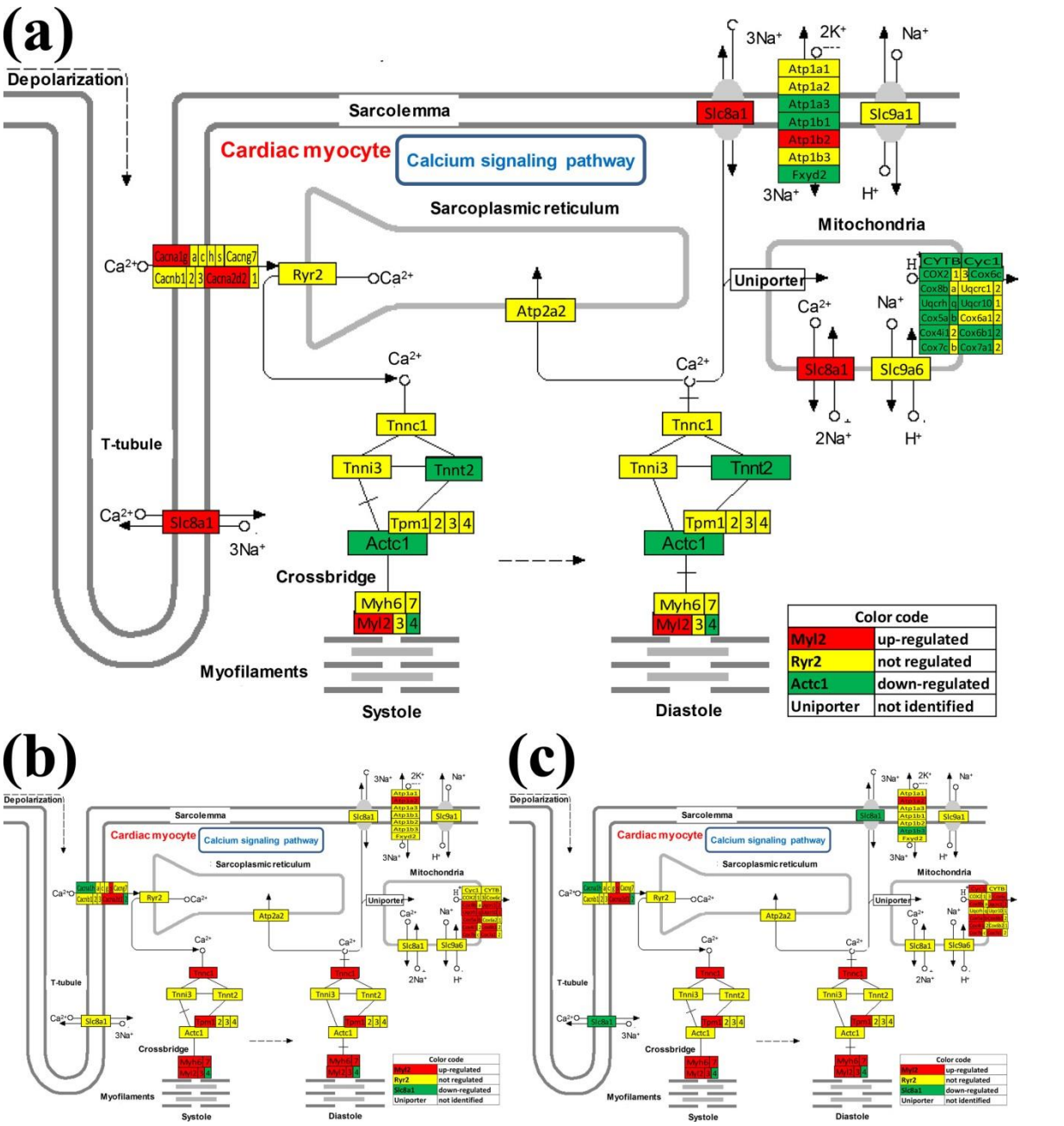

Figure A1: KEGG map (mmu04260) of the differential expression of cardiac muscle contraction (CMC) genes in: (a) the right atrium with respect to the left atrium, (b) left ventricle vs left atrium and (c) right ventricle vs right atrium. No significant difference was found between the expressions of CMC genes in the two ventricles. **Genes with significant differences:** actin alpha cardiac muscle 1 (*Actc1*), Na+/K+ transporting ATPases (*Atp1a2*, *Atp1a*), Ca^{++} transporting ATPases (*Atp1b1*, *Atp1b2*), calcium channels (*Cacna1g*, *Cacna1h*, *Cacna1s*, *Cacna2d1*, *Cacna2d2*), cytochromes c1 and b (*Cyc1*, *Cytb*), cytochrome c oxidases (*Cox2*, *Cox3*, *Cox4i1*, *Cox4i2*, *Cox5a*, *Cox5b*, *Cox6a2*, *Cox6a2*, *Cox6b1*, *Cox6b2*, *Cox6c*, *Co7a1*, *Cox7b*, *Cox7c*, *Cox8b*), FXYD domain-containing ion transport regulator 2 (*Fxyd2*), myosins (*Myh6*, *Myh7*, *Myl2*, *Myl3*, *Myl4*), solute carrier family 8 (sodium/calcium exchanger) member 1 (*Slc8a1*), tropomyosin 1, alpha (*Tpm1*) and troponins (*Tnnc1*, *Tnnt1*).

Preprints (www.preprints.org) | NOT PEER-REVIEWED | Posted: 20 November 2019 doi:10.20944/preprints201911.0243.v1

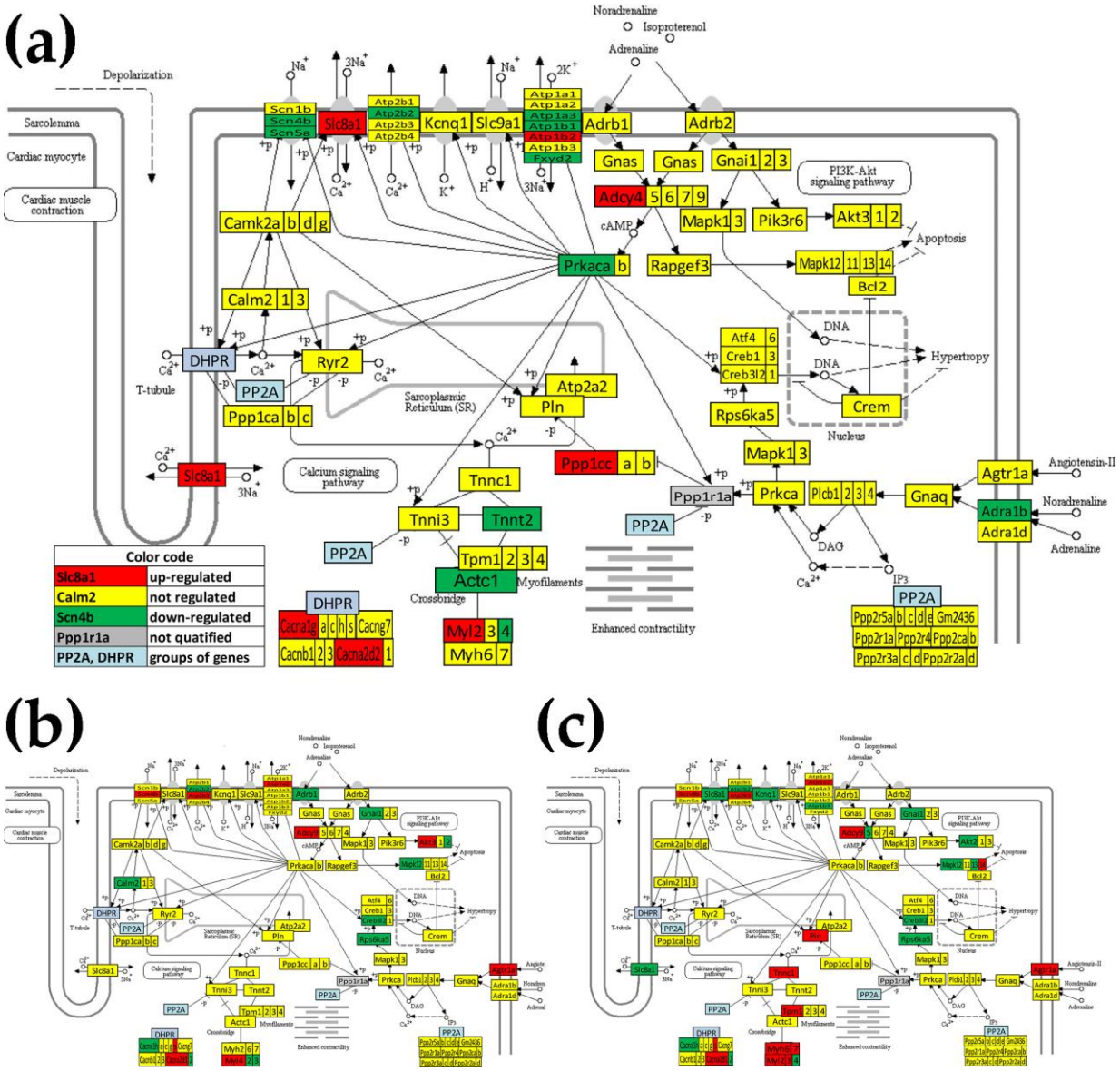

Figure A2: KEGG map (mmu04261) of the differential expression of adrenergic signaling in cardiomyocytes (ASC) genes in: (a) the right atrium with respect to the left right atrium; (b) the left ventricle with respect to the left atrium; (c) the right ventricle with respect to the right atrium. No gene was differentially expressed between the two ventricles. Genes with significant differences: actin, alpha, cardiac muscle 1 (*Actc1*), adenylate cyclases (*Adcy4, Adcy5, Adcy9*), adrenergic receptor, alpha 1b (*Adra1b*), angiotensin (*Agt*), angiotensin II receptor, type 1a (*Agtr1a*), thymoma viral proto-oncogenes (*Akt2, Akt3*), Na^+/K^+-transporting ATPases (*Atp1a2, ATP1a3, ATP1b1, Atp1b3*), Ca^{2+}-transporting ATPases (*Atp2b2, Atp2b3*), calcium channels (*Cacna1g, Cacna1h, Cacna1s, Cacna2d1*), calmodulin 2 (*Calm2*), cAMP responsive element binding protein 3-like 1 (*Creb3l2*), FXYD domain-containing ion transport regulator 2 (*Fxyd2*), guanine nucleotide binding protein (G protein), alpha inhibiting 1 (*Gnai1*), potassium voltage-gated channel subfamily Q member 1 (*Kcnq1*), mitogen-activated protein kinases (*Mapk12, Mapk13, Mapk14*), myosins (*Myh6, Myh7, Myl2, Myl3, Myl4*), phospholamban (*Pln*), protein phosphatases (*Ppp1cc, Ppp1r1b*), protein kinase, cAMP dependent, catalytic, alpha (*Prkaca*), *Rps6ka5*, sodium channels (*Scn4b, Scn5g*), solute carrier family 8 (sodium/calcium exchanger) member 1 (*Slc8a1*), troponins (*Tnnc1, Tnnt2*) and tropomyosin 1 alpha (*Tpm1*).

Table S1. Ratios of RV/LV and RA/LA gene expression in our study for 12 genes encoding subunits of cardiac ion channels and transporters

 doi:10.20944/preprints201911.0243.v1

Gene	Protein	RV/ LV expression ratio	RA / LA expression ratio
Scn5a	Cardiac fast voltage-dependent Na^+ channel main subunit Nav1.5	0.712	0.636
Kcnd2	Cardiac fast transient outward K^+ channel main subunit Kv4.2	1.501	0.694
Kcna4	Cardiac slow transient outward K^+ channel main subunit Kv1.4	1.232	0.953
Clcn2	Voltage-gated chloride channel ClC-2	1.055	0.707
Cacna1c	Cardiac L-type Ca^{2+} channel main subunit Cav1.2	1.087	0.832
Kcnj2	Cardiac inward rectifier K^+ channel main subunit Kir2.1	1.179	0.963
Kcna5	Cardiac ultrarapid delayed rectifier K^+ channel main subunit Kv1.5	0.891	1.018
Kcnh2	Cardiac rapid delayed rectifier K^+ channel main subunit Kv11.1	1.103	1.253
Kcnq1	Cardiac slow delayed rectifier K^+ channel main subunit Kv7.1	0.865	1.117
Atp2a2	Cardiac sarco/endoplasmic reticuluml Ca^{2+} pump main subunit SERCA2	1.199	1.036
Atp1a1	Cardiac Na^+/K^+ pump catalytic subunit $\alpha 1$	0.973	0.890
Slc8a1	Cardiac Na^+/Ca^{2+} antiport exchanger NCX1 main sunbunit	0.895	5.269

References

1. Iacobas, D.A.; Iacobas, S.; Thomas, N.; Spray, D.C. Sex-dependent gene regulatory networks of the heart rhythm. *Funct Integr Genomics* **2010,** *10(1)*:73-86. doi: 10.1007/s10142-009-0137-8.
2. Thomas, N.M.; Jasmin, J.F.; Lisanti, M.P.; Iacobas, D.A. Sex Differences in Expression and subcellular Localization of Heart Rhythm Determinant Proteins. *Biochem Biophys Res Commun* **2011,** *406(1)*:117-22. doi: 10.1016/j.bbrc.2011.02.006.
3. Said, S. I.; Hamidi, S.A.; Dickman, K.G.; Szema, A.M.; Lyubsky, S.; Lin, R.Z.; Jiang, Y.P.; Chen, J.J.; Waschek, J.A.; Kort, K. Moderate Pulmonary Arterial Hypertension in Male Mice Lacking the Vasoactive Intestinal Peptide Gene. *Circulation* **2007**, *115(10)*: 1260-8. doi: 10.161/CIRCULATIONAHA.106.681718.
4. Campen, M. J.; Shimoda, L.A.; O'Donnell, C.P. Acute and Chronic Cardiovascular Effects of Intermittent Hypoxia in C57bl/6j Mice. *J Appl Physiol* **1985**, *99*(5):2028-35. doi: 10.1152/japplphysiol.00411.2005.
5. Reddy, S.; Bernstein, D. Molecular Mechanisms of Right Ventricular Failure. *Circulation* **2015**, *132(18)*: 1734-42. doi: 10.1161/CIRCULATIONAHA.114.012975. Review.
6. Thomas, A.M.; Cabrera, C.P.; Finlay, M.; Lall, K.; Nobles, M.; Schilling, R.J.; Wood, K.; Mein, C.A.; Barnes, M.R.; Munroe, P.B.; Tinker, A. Differentially expressed genes for atrial fibrillation identified by RNA sequencing from paired human left and right atrial appendages. *Physiol Genomics* **2019**, *51(8)*:323-332. doi: 10.1152/physiolgenomics.00012.2019.
7. Karakaya, C.; Goktas, S.; Celik, M.; Kowalski, W.J..; Keller, B.B.; Pekkan, K. Asymmetry in Mechanosensitive Gene Expression during Aortic Arch Morphogenesis. *Sci Rep* **2018**, *8(1):16948*. doi: 10.1038/s41598-018-35127-7.
8. Uosaki, H.; Cahan, P.; Lee, D.I.; Wang, S.; Miyamoto, M.; Fernandez, L.; Kass, D.A.; Kwon, C. Transcriptional Landscape of Cardiomyocyte Maturation. *Cell Rep* **2015,** *13(8): 1705-16*. doi: 10.1016/j.celrep.2015.10.032.
9. Parikh, A.; Wu, J.; Blanton, R.M.; Tzanakakis, E.S. Signaling Pathways and Gene Regulatory Networks in Cardiomyocyte Differentiation. *Tissue Eng Part B Rev* **2015,** *21(4)*:377-92.
10. Dupays, L.; Mohun, T. Spatiotemporal Regulation of Enhancers During Cardiogenesis. *Cell Mol Life Sci* **2016,** *2016*:6.
11. Kathiriya, I.S.; Nora, E.P.; Bruneau, B.G. Investigating the Transcriptional Control of Cardiovascular Development. *Circ Res* **2015,** *116(4)*:700-14.
12. Wamstad, J.A.; Wang, X.; Demuren, O.O.; Boyer, L.A. Distal Enhancers: New Insights into Heart Development and Disease. *Trends Cell Biol* **2014,** *24(5)*:294-302.
13. Fuller, A.M.; Qian, L. Miriad Roles for Micrornas in Cardiac Development and Regeneration. *Cells.* **2014,** *3(3)*:724-50. doi: 10.3390/cells3030724.
14. Yan, S.; Jiao, K. Functions of Mirnas During Mammalian Heart Development. *Int J Mol Sci* **2016,** *17(5)*:E789. doi: 10.3390/ijms17050789.
15. Chen, X.; Chakravarty, T.; Zhang, Y.; Li, X.; Zhong, J.F.; Wang, C. Single-Cell Transcriptome and Epigenomic Reprogramming of Cardiomyocyte-Derived Cardiac Progenitor Cells. *Sci Data* **2016,** *3(160079)*:79.
16. Hirokawa, N.; Tanaka, Y.; Okada, Y.; Takeda, S. Nodal Flow and the Generation of Left-Right Asymmetry. *Cell* **2006,** *125(1)*:33-45. doi: 10.1016/j.cell.2006.03.002.
17. McGrath, J.; Somlo, S.; Makova, S.; Tian, X.; Brueckner, M. Two Populations of Node Monocilia Initiate Left-Right Asymmetry in the Mouse. *Cell* **2003,** *114(1)*:61-73.
18. Komatsu, Y.; Mishina, Y. Establishment of Left-Right Asymmetry in Vertebrate Development: The Node in Mouse Embryos. *Cell Mol Life Sci* **2013,** *70(24)*:4659-66.
19. Takao, D.; Nemoto, T.; Abe, T.; Kiyonari, H.; Kajiura-Kobayashi, H.; Shiratori, H.; Nonaka, S. Asymmetric Distribution of Dynamic Calcium Signals in the Node of Mouse Embryo During Left-Right Axis Formation. *Dev Biol* **2013,** *376(1)*:23-30.
20. Yoshiba, S.; Hamada, H. Roles of Cilia, Fluid Flow, and Ca2+ Signaling in Breaking of Left-Right Symmetry. *Trends Genet* **2014,** *30(1)*:10-7.
21. Yoshiba, S.; Shiratori, H.; Kuo, I.Y.; Kawasumi, A.; Shinohara, K.; Nonaka, S.; Asai, Y.; Sasaki, G.; Belo, J.A.; Sasaki, H.; Nakai, J.; Dworniczak, B.; Ehrlich, B.E.; Pennekamp, P.; Hamada, H. Cilia at the Node of Mouse Embryos Sense Fluid Flow for Left-Right Determination Via Pkd2. *Science* **2012,** *338(6104)*:226-31.
22. Mori, A.D.; Zhu, Y.; Vahora, I.; Nieman, B.; Koshiba-Takeuchi, K.; Davidson, L.; Pizard, A.; Seidman, J.G.; Seidman, C.E.; Chen, X.J.; Henkelman, R.M.; Bruneau, B.G. Tbx5-Dependent Rheostatic Control of Cardiac Gene Expression and Morphogenesis. *Dev Biol.* **2006,** *297(2)*:566-86.

23. Koshiba-Takeuchi, K.; Mori, A.D.; Kaynak, B.L.; Cebra-Thomas, J.; Sukonnik, T.; Georges, R.O.; Latham, S.; Beck, L.; Henkelman, R.M.; Black, B.L.; Olson, E.N.; Wade, J.; Takeuchi, J.K.; Nemer, M.; Gilbert, S.F.; Bruneau, B.G. Reptilian Heart Development and the Molecular Basis of Cardiac Chamber Evolution. *Nature* **2009,** *461(7260)*:95-8. doi: 10.1038/nature08324.
24. Ocaña, O.H.; Coskun, H.; Minguillón, C.; Murawala, P.; Tanaka, E.M.; Galcerán, J.; Muñoz-Chápuli, R.; Nieto, M.A. A Right-Handed Signalling Pathway Drives Heart Looping in Vertebrates. *Nature* **2017,** *549(7670)*:86-90.
25. Borghetti, G.; Eisenberg, C.A.; Signore, S.; Sorrentino, A.; Kaur, K.; Andrade-Vicenty, A.; Edwards, J.G.; Nerkar, M.; Qanud, K.; Sun, D.; Goichberg, P.; Leri, A.; Anversa, P.; Eisenberg, L.M.; Jacobson, J.T.; Hintze, T.H.; Rota, M. Notch Signaling Modulates the Electrical Behavior of Cardiomyocytes. *Am J Physiol Heart Circ Physiol* **2018,** *314(1)*:H68-H81.
26. Koenig, S.N.; Mohler, P.J. The evolving role of ankyrin-B in cardiovascular disease. *Heart Rhythm* **2017**, 14(12):1884-1889. doi: 10.1016/j.hrthm.2017.07.032.
27. Lee, P.R.; Cohen, J.E.; Iacobas, D.A.; Iacobas, S.; Fields, R.D. Gene networks activated by pattern-specific generation of action potentials in dorsal root ganglia neurons. *Sci Rep* **2017**, **7**:43765, doi:10.1038/srep43765.
28. Iacobas, D.A.; Iacobas, S.; Lee, P.R.; Cohen, J.E.; Fields, R.D. Coordinated activity of transcriptional networks responding to the pattern of action potential firing in neurons. *Genes* **2019**, 10, 754; doi:10.3390/genes10100754.
29. Iacobas, S.; Ede, N.; Iacobas, D.A. The Gene Master Regulators (GMR) Approach Provides Legitimate Targets for Personalized, Time-Sensitive Cancer Gene Therapy. *Genes* **2019**, *10*(8), 560. doi:10.3390/genes10080560.
30. Iacobas, D.A.; Iacobas, S.; Tanowitz, H.B.; deCarvalho, A.C.; Spray, D.C. Functional genomic fabrics are remodeled in a mouse model of Chagasic cardiomyopathy and restored following cell therapy. *Microbes Infect* **2018**, *20*(3), 185-195. doi: 10.1016/j.micinf.2017.11.003.
31. Iacobas, D.A.; Fan, C.; Iacobas, S.; Haddad, G.G. Integrated transcriptomic response to cardiac chronic hypoxia: translation regulators and response to stress in cell survival. *Funct Integr Genomics* **2008,** *8*(3):265-75. doi: 10.1007/s10142-008-0082-y.
32. Iacobas, D.A.; Iacobas, S.; Haddad, G.G. Heart rhythm genomic fabric in hypoxia. *Biochem Biophys Res Commun* **2010**, *391*(4):1769-1774. doi: 10.1016/j.bbrc.2009.12.151.
33. Adesse, D.; Goldenberg, .R.;, Fortes, F.S.; Iacobas, D.A.; Iacobas, S.; Campos de Carvalho, A.C.; de Nararetth, M.; Huang, H.; Tanowitz, H.B.; Garzoni, L.R.; Spray, D.C. Gap junctions and Chagas' disease. *Adv Parasitol* **2011**, *76*: 63-81. doi: 10.1016/B978-0-12-385895-5.00003-7.
34. Iacobas, D.A.; Iacobas, S.; Li, W.E.; Zoidl, G.; Dermietzel, R.; Spray, D.C. Genes controlling multiple functional pathways are transcriptionally regulated in connexin43 null mouse heart. *Physiol Genomics* **2005**, *20*: 211-223. DOI:10.1152/physiolgenomics.00229.2003.
35. Amuzescu, B.; Maniu, H. Molecular and Cellular Biology of the Right Heart. In *Right Heart Pathology. From Mechanism to Management*, edited by S. Dumitrescu, Tintoiu, I. C., Underwood, M. J., 57-89. New York: Springer Nature, **2018**.
36. Anderson, C.; Khan, M.A.; Wong, F.; Solovieva, T.; Oliveira, N.M.; Baldock, R.A.; Tickle, C.; Burt, D.W.; Stern, C.D. A Strategy to Discover New Organizers Identifies a Putative Heart Organizer. *Nat Commun* **2016,** *7*:12656.
37. Lescroart, F.; Chabab, S.; Lin, X.; Rulands, S.; Paulissen, C.; Rodolosse, A.; Auer, H.; Achouri, Y.; Dubois, C.; Bondue, A.; Simons, B.D.; Blanpain, C. Early Lineage Restriction in Temporally Distinct Populations of Mesp1 Progenitors During Mammalian Heart Development. *Nat Cell Biol* **2014,** *16(9)*:829-40.
38. Lescroart, F.; Wang, X.; Lin, X.; Swedlund, B.; Gargouri, S.; Sànchez-Dànes, A.; Moignard, V.; Dubois, C.; Paulissen, C.; Kinston, S.; Göttgens, B.; Blanpain, C. Defining the Earliest Step of Cardiovascular Lineage Segregation by Single-Cell Rna-Seq. *Science* **2018,** *359(6380)*:1177-81.
39. Wamstad, J.A.; Alexander, J.M.; Truty, R.M.; Shrikumar, A.; Li, F.; Eilertson, K.E.; Ding, H.; Wylie, J.N.; Pico, A.R.; Capra, J.A.; Erwin, G.; Kattman, S.J.; Keller, G.M.; Srivastava, D.; Levine, S.S.; Pollard, K.S.; Holloway, A.K.; Boyer, L.A.; Bruneau, B.G. Dynamic and Coordinated Epigenetic Regulation of Developmental Transitions in the Cardiac Lineage. *Cell* **2012,** *151(1)*:206-20.
40. Wang, L.; Morotti, S.; Tapa, S.; Francis Stuart, S.D.; Jiang, Y.; Wang, Z.; Myles, R.C.; Brack, K.E.; Ng, G.A.; Bers, D.M.; Grandi, E.; Ripplinger, C.M. Different Paths, Same Destination: Divergent Action Potential Responses Produce Conserved Cardiac Fight-or-Flight Response in Mouse and Rabbit Hearts. *J Physiol* **2019,** *597(15)*:3867-83.
41. Iacobas, S.; Iacobas, D.A. Astrocyte proximity modulates the myelination gene fabric of oligodendrocytes. *Neuron Glia Biol* **2010**, 6(3): 157-169. doi: 10.1017/S1740925X10000220
42. Iacobas, S.; Thomas, N.M.; Iacobas, D.A. Plasticity of the myelination genomic fabric. *Mol Genet Genomics* **2012**, 287(3):237-46. doi: 10.1007/s00438-012-0673-0